


Generalized Hydrodynamics on an Atom Chip

M. Schemmer,¹ I. Bouchoule,¹ B. Doyon,² and J. Dubail³

¹Laboratoire Charles Fabry, Institut d'Optique, CNRS, Université Paris-Saclay, 91127 Palaiseau cedex, France

²Department of Mathematics, King's College London, Strand, London WC2R 2LS, United Kingdom

³Laboratoire de Physique et Chimie Théoriques, CNRS, Université de Lorraine, UMR 7019, F-54506 Vandoeuvre-les-Nancy, France

 (Received 24 October 2018; revised manuscript received 12 December 2018; published 5 March 2019)

The emergence of a special type of fluidlike behavior at large scales in one-dimensional (1D) quantum integrable systems, theoretically predicted in O. A. Castro-Alvaredo *et al.*, Emergent Hydrodynamics in Integrable Quantum Systems Out of Equilibrium, *Phys. Rev. X* **6**, 041065 (2016) and B. Bertini *et al.*, Transport in Out-of-Equilibrium XXZ Chains: Exact Profiles of Charges and Currents, *Phys. Rev. Lett.* **117**, 207201 (2016), is established experimentally, by monitoring the time evolution of the *in situ* density profile of a single 1D cloud of ⁸⁷Rb atoms trapped on an atom chip after a quench of the longitudinal trapping potential. The theory can be viewed as a dynamical extension of the thermodynamics of Yang and Yang, and applies to the whole range of repulsive interaction strength and temperature of the gas. The measurements, performed on weakly interacting atomic clouds that lie at the crossover between the quasicondensate and the ideal Bose gas regimes, are in very good agreement with the theory. This contrasts with the previously existing “conventional” hydrodynamic approach—that relies on the assumption of local thermal equilibrium—which is unable to reproduce the experimental data.

DOI: [10.1103/PhysRevLett.122.090601](https://doi.org/10.1103/PhysRevLett.122.090601)

The emergent hydrodynamic behavior of many interacting particles is a fascinating phenomenon: at the atomic level, all quantum (classical) systems are described by the Schrödinger (Newton) equation, yet these unique microscopic descriptions give rise to a wealth of different liquid and gas phases at larger scales, from the ideal gas to liquid water to plasmas to superfluid helium to Bose-Einstein condensates, to name but a few. Inferring the correct hydrodynamic behavior directly from the microscopic constituents of a many-body system is, in general, a very ambitious task that typically involves extensive numerical simulations and a hierarchy of different modelings on intermediate scales [1,2].

However, there exist a few simpler systems where the emergence of a special kind of hydrodynamics can be linked directly to the underlying microscopic rules [3]. One such system is the one-dimensional (1D) classical billiard, or hard-rod gas [3–5], whose hydrodynamic behavior, as seen below, is similar to that of the quantum system studied in this Letter. The hard-rod gas consists of N identical impenetrable rods of fixed diameter Δ that move along a line, and exchange their momenta upon colliding elastically. At large N , the 1D billiard admits a hydrodynamic description: in the limit of density variations of very long wavelength, the billiard can be described by a continuous distribution $\rho(x, v)$ of rods moving at velocity v around a position x and this distribution satisfies an exact evolution equation which resembles the Liouville equation for phase space densities, up to a renormalization of the bare velocity

v [see Eq. (2)]. The latter renormalization encodes the following microscopic mechanism: when one rod with velocity v hits another one with velocity $w < v$ from the left, they exchange their momenta. Equivalently, because all the rods are identical, one can think of the collision as an instantaneous exchange of their positions, as if the rod with bare velocity v jumped instantaneously by a distance Δ to the right. Thus, the time needed by that rod to travel a distance ℓ is not ℓ/v , but rather $(\ell - \Delta)/v$. For a finite density of rods, this results in each rod with bare velocity v moving at an effective velocity $v^{\text{eff}}(v)$, that depends on the distribution $\rho(x, v)$ [3–5]. In distributions of long wavelengths, the evolution equation for $\rho(x, v)$ becomes a hydrodynamic flow controlled by the local effective velocity v^{eff} . The 1D billiard thus exhibits an interesting hydrodynamic behavior that is straightforwardly related to its microscopics. Slight generalizations of that model exist, where the jumping distance Δ depends on the relative velocity $v - w$, which possess a similar hydrodynamic description [6].

Remarkably, the *same* emergent hydrodynamics was rediscovered in 2016 in the context of 1D quantum integrable models [7,8]—the resulting theoretical framework is now dubbed generalized hydrodynamics (GHD). Cold atom experiments offer a unique platform to test the validity of this theoretical breakthrough. Indeed 1D clouds are well described by the 1D Bose gas with contact repulsion [9–11], a paradigmatic integrable system known as the Lieb-Liniger model [12] whose large-scale dynamics

is argued to be given by GHD [7,13–22]. Many other integrable models are argued to be described by GHD, leading to intense research activity in the past two years [8,23–32].

The goal of this Letter is to establish *experimentally* GHD as the correct hydrodynamic description of the 1D Bose gas. To do so, we measure the *in situ* density profiles of a time-evolving 1D atomic cloud trapped on an atom chip, and compare the data with predictions from GHD. We contrast those predictions with the ones of the conventional hydrodynamic (CHD) approach—based on the assumption of local thermal equilibrium [33]—that has been frequently used [34–39]. Starting from a cloud at thermal equilibrium in a longitudinal potential $V(x)$, dynamics is triggered by suddenly quenching $V(x)$. We consider three types of quenches. The first is a 1D expansion of the cloud from an initial harmonic potential (Fig. 1); the second is a 1D expansion from a double-well potential (Fig. 3); the third is a quench from double-well to harmonic potential (Fig. 4). We find that only GHD is able to accurately describe the time evolution of the cloud beyond the harmonic case.

Generalized hydrodynamics.—The Hamiltonian that describes our atomic gas of N bosons of mass m confined in a potential $V(x)$ with contact repulsion is

$$H = -\frac{\hbar^2}{2m} \sum_{i=1}^N \partial_{x_i}^2 + g \sum_{i<j} \delta(x_i - x_j) + \sum_{i=1}^N V(x_i), \quad (1)$$

which reduces to the model solved by Lieb and Liniger [12] when $V(x) = 0$. As in any hydrodynamic approach, the idea is to trade that microscopic model for a simpler, long-wavelength, description in terms of continuous densities.

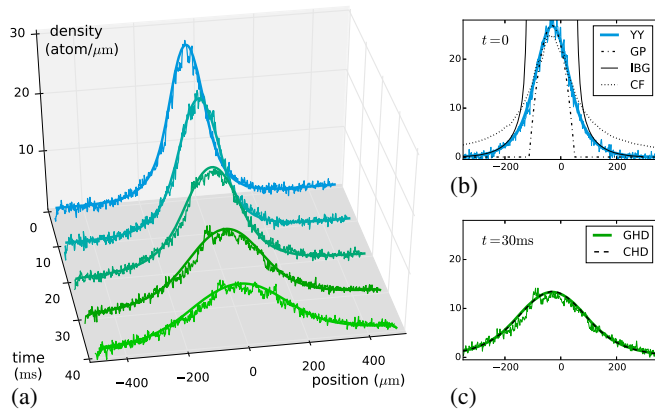


FIG. 1. (i) *In situ* density profile after longitudinal expansion from a harmonic trap of a 1D cloud of $N = 4600 \pm 100$ ^{87}Rb atoms; the smooth curve is the theoretical prediction of GHD and the noisy one is the experimental data. (ii) Initial profile obtained from the Yang-Yang equation of state (YY), Gross-Pitaevskii, ideal Bose gas, and classical field [40], with the same temperature and chemical potential as for YY. (iii) Evolution from the YY initial profile with GHD and conventional hydrodynamics.

The fluid consists of local “fluid cells” of size δx , with δx very short compared to the wavelength of density variations, but very long compared to microscopic lengths in the gas. The state inside each local fluid cell $[x, x + \delta x]$ is a macrostate of the Lieb-Liniger model that is entirely characterized by its distribution $\rho(x, v)$ of rapidities v , similarly to the celebrated thermodynamic Bethe ansatz of Yang and Yang [46,47] (as explained in Refs. [7,8], that these are the correct local macrostates can be seen as a consequence of recent results on “generalized thermalization” [48,49]). Semiclassically, one may view the rapidity v as the bare velocity of a *quasiparticle*. As in the 1D billiard, the velocity v gets renormalized in the presence of other quasiparticles, resulting in an effective velocity that is the solution of an integral equation [3,5,7,8],

$$v^{\text{eff}}(v) = v + \int dw \rho(w) \Delta(v-w) [v^{\text{eff}}(v) - v^{\text{eff}}(w)]. \quad (2a)$$

However, while in the classical billiard the jumping distance $\Delta(v-w)$ at each collision is a constant—the length of the rods—in the Bose gas it corresponds to the time delay resulting from the two-body scattering phase $\phi(v-w)$ through differentiation [12], $\Delta(v-w) = -(\hbar/m) \times \{[d\phi(v-w)]/[d(v-w)]\}$. This gives $\Delta(v-w) = -\{(2g/m)/[(g/\hbar)^2 + (v-w)^2]\}$ for the Dirac delta potential (see Ref. [6] for an extended discussion). The effective velocity enters the evolution equation for the distribution $\rho(x, v)$ as follows [7,8,13]:

$$\partial_t \rho + \partial_x [v^{\text{eff}} \rho] = \left(\frac{\partial_x V}{m} \right) \partial_v \rho. \quad (2b)$$

This resembles a Liouville equation for phase space densities of quasi-particles, although it is to be stressed that it is a Euler hydrodynamic equation, determining the evolution of the degrees of freedom emerging at large wavelengths. GHD consists of Eqs. (2a) and (2b). In practice, for a given initial distribution $\rho(x, v)$, the GHD equations can be efficiently solved numerically [6,14,17,19]; in this Letter we rely on a finite-difference method similar to the one discussed in Ref. [19]. Importantly, for our purposes, the atomic density $n(x)$ is obtained from the distribution $\rho(x, v)$ by integrating locally over all rapidities, $n(x) = \int dv \rho(x, v)$.

The atom chip.—Our experimental setup is described in detail in Ref. [50]. ^{87}Rb atoms are confined in a magnetic trap produced by microwires deposited on the surface of a chip. The transverse confinement is provided by three 1.3 mm long parallel wires (red wires in Fig. 2), which carry ac currents modulated at 400 kHz: atoms are guided along x , at a distance of $12\mu\text{m}$ above the central wire, with a transverse frequency ω_{\perp} which lies between 5 and 8 kHz. The modulation technique permits an independent control of the longitudinal potential $V(x)$, which is realized by two

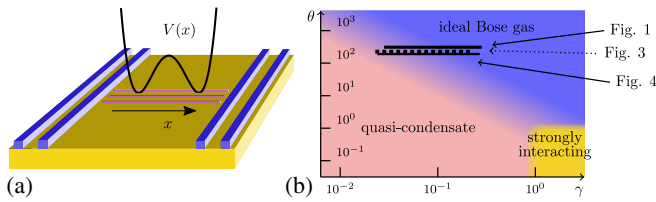


FIG. 2. (a) The atom chip setup with the four wires (blue) creating the longitudinal potential and the three wires (red) creating the strong transverse confinement. (b) Position of our three data sets in the thermal equilibrium phase diagram of the Lieb-Liniger gas with $\gamma = mg/(\hbar^2 n)$ and $\theta = 2\hbar^2 k_B T / (mg^2)$ [51]. At the center of the cloud γ is of order 10^{-2} , but it increases in the wings as the density decreases; we display the segments $[\gamma_{\min}, \gamma_{\min}/10]$ corresponding to a local density $n(x)$ not smaller than a tenth of the maximal density in the cloud. The asymptotic regimes of the Lieb-Liniger gas, separated by smooth crossovers, are shown in colors. Our data sets lie at the crossover between the quasicondensate and the ideal Bose gas regimes.

pairs of wires perpendicular to x , running dc current (blue wires in Fig. 2). The atomic cloud is far from those wires, in a region where $V(x)$ is well approximated by its Taylor expansion at small x . By tuning the currents in the four wires, we effectively control the coefficients of the x , x^2 , x^3 , and x^4 terms in that expansion: we can thus produce harmonic potentials, but also double-well potentials.

Using radio-frequency evaporative cooling we produce cold atomic clouds in the 1D regime, with a typical energy per atom smaller than the transverse energy gap: the temperature and chemical potential fulfill $k_B T, \mu < \hbar\omega_{\perp}$. The gas is then well described by the 1D model (1), with the effective 1D repulsion strength $g = 2\hbar a\omega_{\perp}$ [52], where the 3d scattering length of ^{87}Rb is $a = 5.3$ nm, and the mass is $m = 1.43 \times 10^{-25}$ kg. Moreover the length scale on which $n(x)$ varies is much larger than microscopic lengths—the phase correlation length at thermal equilibrium, which is the largest microscopic length in the quasicondensate regime, is of order $n\hbar^2/(mk_B T)$ [53,54], typically $0.1 \mu\text{m}$ for our clouds—so the hydrodynamic description applies. At equilibrium, the latter is equivalent to the local density approximation (LDA), and the local properties of the gas are parametrized by the dimensionless repulsion strength $\gamma = mg/(\hbar^2 n)$ and the dimensionless temperature $\theta = 2\hbar^2 k_B T / (mg^2)$ [51]. The range (γ, θ) explored by our data sets is displayed in Fig. 2(b). In this Letter we analyze the density profiles $n(x)$, which we measure using absorption images [50], averaging over typically ten images, with a pixel size of $1.74 \mu\text{m}$ in the atomic plane.

The Yang-Yang initial profile.—We start by trapping a cloud of $N = 4600 \pm 100$ atoms, with $\omega_{\perp} = 2\pi \times (7.75 \pm 0.02)$ kHz, in a harmonic potential $V(x) = m\omega_{\parallel}^2 x^2 / 2$ with $\omega_{\parallel} = 2\pi \times (8.8 \pm 0.04)$ Hz, and measure its density profile [Fig. 1(b)]. To evaluate the temperature of the cloud, we fit the experimental profile with the one predicted by the Yang-Yang equation of state [9–11,46], relying on LDA

and on the assumption that the cloud is at thermal equilibrium; we find $T = (0.43 \pm 0.013) \mu\text{K}$. This gives $\theta = (3.5 \pm 0.1) \times 10^2$, while the interaction parameter is $\gamma = (2.8 \pm 0.1) \times 10^{-2}$ at the center.

As the density varies from the center of the cloud to the wings, the gas locally explores several regimes [51], from quasicondensate to highly degenerate ideal Bose gas (IBG) to nondegenerate IBG; see Fig. 2(b). The Yang-Yang equation of state [46] is exact in the entire phase diagram of the Lieb-Liniger model, and thus faithfully describes the density profile within LDA. We stress that this is the most natural and powerful method to describe the initial state of the gas [9–11], and that no simpler approximate theory [40] can account for the whole initial density profile; see Fig. 1(b). The Gross-Pitaevskii (GP) theory works in the central part—because it is close to the quasicondensate regime, but not in the wings. The opposite is true for the IBG model: it correctly describes the wings, but not the center of the cloud—the chemical potential is positive in the center, so the density diverges in the IBG. The classical field theory captures the quasicondensation transition for gases deep in the weakly interacting regime but it fails to reproduce faithfully the wings of our cloud since the latter are not highly degenerate.

Expansion from harmonic trap: Agreement with both GHD and CHD.—At $t = 0$, we suddenly switch off the longitudinal harmonic potential $V(x)$, and let the cloud expand freely in one dimension. We measure the *in situ* profiles at times $t = 10, 20, 30$ and 40 ms; see Fig. 1(a).

Two theories are able to give predictions for the expansion starting from the locally thermal initial state. One is GHD, presented above, where the full distribution of quasiparticles $\rho(x, v)$ is evolved in time [55]. The other is the *conventional* hydrodynamics (CHD) of the gas which, contrary to GHD, assumes that all local fluid cells are at thermal equilibrium, and keeps track only of three quantities that entirely describe the local state of the gas: the density $n(x)$, the fluid velocity $u(x)$, and the internal energy $e(x)$ [40]. We calculate the evolution of the density profile with both theories, and find that both of them are in excellent agreement with the experimental data, see Fig. 1(c) for the result at $t = 30$ ms.

GHD and CHD thus appear to be indistinguishable in that situation, at least for the expansion times that we probe here. We attribute this coincidence to the initial *harmonic* potential, which is very special. In this case it is simple to see that the GHD and CHD predictions coincide in the ideal Bose gas regime, and they can be shown to stay relatively near even beyond that regime [56].

Discussion: GHD vs CHD.—We wish to identify a setup where the theoretical predictions of both theories clearly differ, in order to experimentally discriminate between them. This will be the case if GHD predicts, for some time t and at some position x , that the distribution of rapidities $\rho(x, v)$ will differ strongly from a thermal equilibrium one.

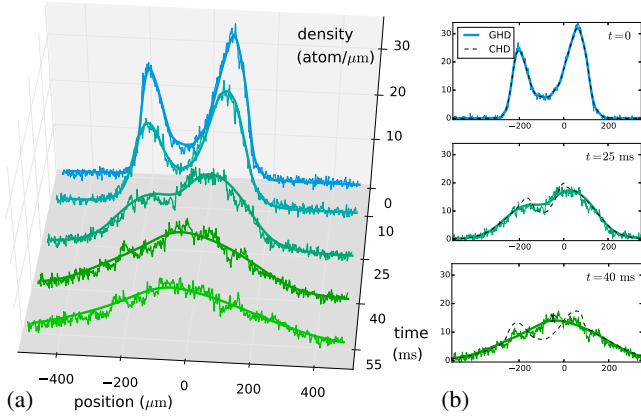


FIG. 3. (i) Longitudinal expansion of a cloud of $N = 6300 \pm 200$ atoms initially trapped in a double-well potential, compared with GHD. (ii) Even though the initial state is the same for GHD and CHD, both theories clearly differ at later times. CHD wrongly predicts the formation of two large density waves. The error bar shown at the center at $t = 40$ ms corresponds to a 68% confidence interval, and is representative for all data sets.

Such a situation occurs during the expansion of a cloud that initially has two well separated density peaks (Fig. 3). The reason can be captured by the following argument. The fluid cells $[x, x + \delta x]$ that are around either of the two peaks contain more quasiparticles, including quasiparticles of large rapidities, than the fluid cells near the center at $x = 0$. Under time evolution, the quasiparticles from the left peak that have a large positive rapidity $+u$ soon meet the ones coming from the right peak that have a large negative rapidity $-u$, around $x = 0$. Then, the distribution of rapidities near $x = 0$ is double peaked, with maxima at $v \simeq \pm u$, so it is clearly very far from a thermal equilibrium distribution, which would be single peaked. This phenomenon is obvious for noninteracting particles, Eq. (2) reducing to the standard Liouville equation, and GHD calculations indicate that this is true also for interacting particles [17,57].

Expansion from a double well.—To realize the above scenario, we prepare a cloud of $N = 6300 \pm 200$ atoms, with $\omega_{\perp} = 2\pi \times (8.1 \pm 0.03)$ kHz, at thermal equilibrium in a longitudinal double-well potential $V(x)$, such that the atomic density presents two well separated peaks, the peak density corresponding to $\gamma = (2.45 \pm 0.07) \times 10^{-2}$. Then at $t = 0$ we suddenly switch off the potential $V(x)$ and measure the *in situ* profiles at time $t = 10, 25, 40, 55$ ms (Fig. 3).

To compare with theoretical predictions, we need to know the initial temperature T of the cloud. However, we cannot estimate T from fitting the initial density profile $n_0(x)$ with the Yang-Yang equation of state and LDA because we do not have a good knowledge of the initial potential $V(x)$ that we create on the chip. Instead, we proceed as follows. First we postulate an initial temperature T and construct the initial rapidity distribution $\rho_T(x, v)$ such that, for a given x , $\rho_T(x, v)$ is the Yang-Yang thermal equilibrium rapidity distribution [46] at temperature T and density $n_0(x)$. We

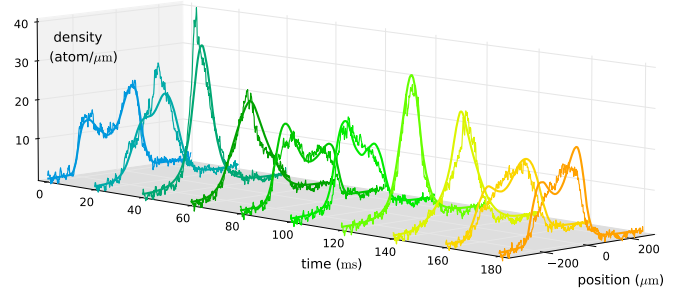


FIG. 4. Quench from double-well to harmonic potential, compared to the GHD prediction, with an atomic cloud that contains $N = 3500 \pm 140$ atoms initially. The main features of the experimental data are well reproduced by GHD. One experimental effect, not modeled in GHD, that appears to be particularly important, are the three-body losses: after 180 ms, the number of atoms drops by approximately 15%.

then evolve $\rho_T(x, v)$ using GHD and compute $n_T(x, t)$. While, by construction, $n_T(x, 0) = n_0(x)$, $n_T(x, t)$ may differ from the data at later times. We repeat this procedure for several initial temperatures and we select the value of T whose time evolution is in best agreement with the data [58]. We obtain $T \simeq 0.3 \mu\text{K}$, corresponding to $\theta \simeq 2 \times 10^2$, see Fig. 2(b).

The comparison between the expansion data and GHD is shown in Fig. 3(a); the agreement is excellent. We also simulate the time evolution of the cloud with CHD, for the exact same initial state. As we expected, expanding from a double-well potential reveals a clear difference between CHD and GHD, see Fig. 3(b). Two large density waves emerge in CHD and large gradients develop, eventually leading to shocks [14], features which are not seen in GHD [57].

Quench from double-well to harmonic potential.—Finally, we trap $N = 3500 \pm 140$ atoms, with $\omega_{\perp} = 2\pi \times (5.4 \pm 0.02)$ kHz, in a double-well potential, and we study the evolution of the cloud after suddenly switching off the double well and replacing it by a harmonic potential of frequency $\omega_{\parallel} = 2\pi \times (6.5 \pm 0.03)$ Hz. We measure the *in situ* profiles at time $t = 0, 20, 40, \dots, 180$ ms; see Fig. 4. The initial peak density corresponds to $\gamma = (2.13 \pm 0.07) \times 10^{-2}$. To estimate the temperature of the cloud, we proceed as in the previous case [58]; we find $T \simeq 0.15 \mu\text{K}$, corresponding to $\theta \simeq 2.2 \times 10^2$ [Fig. 2(b)].

This quench protocol mimics the famous quantum Newton's Cradle experiment [59]—see also Refs. [60,61] for recent realizations—which is realized here in a weakly interacting gas. Exactly like in the previous paragraph, this is a situation where GHD predicts the appearance of non-thermal rapidity distributions [17,62], and must therefore differ strongly from CHD. In fact, we have observed that CHD develops a shock at short times (around $t \simeq 30$ ms), so it is simply unable to give any prediction for the whole evolution time investigated experimentally [63].

Importantly, the motion is not periodic, contrary to what would be seen purely in the IBG or in the strongly interacting fermionized regime. Nevertheless, the motion of the cloud preserves an *approximate* periodicity, with a period close to, but slightly longer than, $2\pi/\omega_{\parallel}$ [62] (of course, if the cloud was symmetric under $x \rightarrow -x$, the period would be divided by two). At a quarter of the period—and three quarters of the period—the density distribution shows a single thin peak located near $x = 0$. We find good agreement with the GHD predictions, with the initial temperature T as the only free parameter [58]. However, experimental effects not taken into account by the GHD equations (2) appear to be more important in this setup than in the previous ones of Figs. 1–3, where shorter times were probed. For instance, the number of atoms N is not constant in our experimental setup: it decreases with time and drops by approximately 15% after 180 ms, probably because of three-body losses that occur at large density. This might partially explain the difference between the experimental density profile and the GHD one. We also suspect the small residual roughness of the potential $V(x)$ of affecting the experimental profiles.

Conclusion.—The results presented in this Letter are the first experimental check of the validity of GHD for 1D integrable quantum systems. We have shown that GHD—which predicts the time evolution of the distribution of rapidities—accurately captures the motion of 1D cold bosonic clouds made of $N \sim 10^3$ atoms, on timescales of up to ~ 0.2 s. We probed situations where the GHD predictions significantly differ from the ones of the conventional hydrodynamic approach, even at short times. We stress that GHD is applicable to all regimes of the 1D Bose gas, and it would therefore be particularly interesting to probe the strongly interacting regime. More generally, GHD is applicable to all Bethe ansatz solvable models, including multicomponent mixtures of fermions and bosons with symmetric interactions [64–67], so it would be very exciting to use it to describe the dynamics of more complex gases that can be realized in experimental setups different from ours [68,69].

We thank R. Dubessy for very stimulating discussions, and M. Cheneau for his careful reading of the manuscript. B. D. and J. D. thank J.-S. Caux, R. Konik, and T. Yoshimura for joint work on closely related projects. M. S. and I. B. thank S. Bouchoule of C2N (Centre Nanosciences et Nanotechnologies, CNRS/UPSUD, Marcoussis, France) for the development and microfabrication of the atom chip. A. Durnez and A. Harouri of C2N are acknowledged for their technical support. C2N laboratory is a member of RENATECH, the French national network of large facilities for micronanotechnology. M. S. acknowledges support by the Studienstiftung des Deutschen Volkes. This work was supported by Région Île de France (DIM NanoK, Atocirc project), and by the CNRS Mission Interdisciplinaire “Défi Infini” (J. D.).

B. D. thanks the Centre for Non-Equilibrium Sciences (CNES) and the Thomas Young Centre (TYC), as well as the Perimeter Institute (Waterloo, Canada) for hospitality while some of this work was done; J. D. also thanks SISSA in Trieste for hospitality. B. D. and J. D. thank the Galileo Galilei Institute for Theoretical Physics (Florence, Italy) for hospitality during the workshop “Entanglement in Quantum Systems,” and the Erwin Schrodinger Institute (Vienna, Austria) for hospitality during the programme “Quantum Paths.”

-
- [1] J.-P. Hansen and I. R. McDonald, *Theory of Simple Liquids*, 2nd ed. (Academic Press, San Diego, CA, 1990).
 - [2] M. P. Allen and D. J. Tildesley, *Computer Simulation of Liquids*, 2nd ed. (Oxford University Press, Oxford, UK, 2017).
 - [3] H. Spohn, *Large Scale Dynamics of Interacting Particles* (Springer, Berlin, 1991).
 - [4] J. K. Percus, Exact solution of kinetics of a model classical fluid, *Phys. Fluids* **12**, 1560 (1969).
 - [5] C. Boldrighini, R. L. Dobrushin, and Yu. M. Sukhov, One-dimensional hard rod caricature of hydrodynamics, *J. Stat. Phys.* **31**, 577 (1983).
 - [6] B. Doyon, T. Yoshimura, and J.-S. Caux, Soliton Gases and Generalized Hydrodynamics, *Phys. Rev. Lett.* **120**, 045301 (2018).
 - [7] O. A. Castro-Alvaredo, B. Doyon, and T. Yoshimura, Emergent Hydrodynamics in Integrable Quantum Systems Out of Equilibrium, *Phys. Rev. X* **6**, 041065 (2016).
 - [8] B. Bertini, M. Collura, J. De Nardis, and M. Fagotti, Transport in Out-of-Equilibrium XXZ Chains: Exact Profiles of Charges and Currents, *Phys. Rev. Lett.* **117**, 207201 (2016).
 - [9] A. H. van Amerongen, J. J. P. van Es, P. Wicke, K. V. Kheruntsyan, and N. J. van Druten, Yang-Yang Thermodynamics on an Atom Chip, *Phys. Rev. Lett.* **100**, 090402 (2008).
 - [10] T. Jacqmin, J. Armijo, T. Berrada, K. V. Kheruntsyan, and I. Bouchoule, Sub-Poissonian Fluctuations in a 1D Bose Gas: From the Quantum Quasicondensate to the Strongly Interacting Regime, *Phys. Rev. Lett.* **106**, 230405 (2011).
 - [11] A. Vogler, R. Labouvie, F. Stubenrauch, G. Barontini, V. Guarrera, and H. Ott, Thermodynamics of strongly correlated one-dimensional Bose gases, *Phys. Rev. A* **88**, 031603(R) (2013).
 - [12] E. H. Lieb and W. Liniger, Exact analysis of an interacting Bose gas. I. The general solution and the ground state, *Phys. Rev.* **130**, 1605 (1963); F. Berezin, G. Pokhil, and V. Finkelberg, Schrödinger equation for a system of 1D particles with point interaction, *Vestn. MGU* **1**, 21 (1964).
 - [13] B. Doyon and T. Yoshimura, A note on generalized hydrodynamics: Inhomogeneous fields and other concepts, *SciPost Phys.* **2**, 014 (2017).
 - [14] B. Doyon, J. Dubail, R. Konik, and T. Yoshimura, Large-Scale Description of Interacting One-Dimensional Bose Gases: Generalized Hydrodynamics Supersedes Conventional Hydrodynamics, *Phys. Rev. Lett.* **119**, 195301 (2017).

- [15] B. Doyon and H. Spohn, Drude weight for the Lieb-Liniger Bose gas, *SciPost Phys.* **3**, 039 (2017).
- [16] V.B. Bulchandani, R. Vasseur, C. Karrasch, and J.E. Moore, Solvable Hydrodynamics of Quantum Integrable Systems, *Phys. Rev. Lett.* **119**, 220604 (2017).
- [17] J.-S. Caux, B. Doyon, J. Dubail, R. Konik, and T. Yoshimura, Hydrodynamics of the interacting Bose gas in the Quantum Newton Cradle setup, [arXiv:1711.0873](https://arxiv.org/abs/1711.0873).
- [18] J. Dubail, A more efficient way to describe interacting quantum particles in 1D, *Viewpoint on Refs.* [7,8] in *Physics* **9**, 153 (2016).
- [19] V.B. Bulchandani, R. Vasseur, C. Karrasch, and J.E. Moore, Bethe-Boltzmann hydrodynamics and spin transport in the XXZ chain, *Phys. Rev. B* **97**, 045407 (2018).
- [20] J. De Nardis, D. Bernard, and B. Doyon, Hydrodynamic Diffusion in Integrable Systems, *Phys. Rev. Lett.* **121**, 160603 (2018).
- [21] D.-L. Vu and T. Yoshimura, Equations of state in generalized hydrodynamics, [arXiv:1809.03197](https://arxiv.org/abs/1809.03197).
- [22] A. Bastianello and L. Piroli, From the sinh-Gordon field theory to the one-dimensional Bose gas: Exact local correlations and full counting statistics, *J. Stat. Mech.* (2018) 113104.
- [23] A. De Luca, M. Collura, and J. De Nardis, Non-equilibrium spin transport in integrable spin chains: Persistent currents and emergence of magnetic domains, *Phys. Rev. B* **96**, 020403 (2017).
- [24] B. Doyon and H. Spohn, Dynamics of hard rods with initial domain wall state, *J. Stat. Mech.* (2017) 073210.
- [25] E. Ilievski and J. De Nardis, Microscopic Origin of Ideal Conductivity in Integrable Quantum Models, *Phys. Rev. Lett.* **119**, 020602 (2017).
- [26] L. Piroli, J. De Nardis, M. Collura, B. Bertini, and M. Fagotti, Transport in out-of-equilibrium XXZ chains: Nonballistic behavior and correlation functions, *Phys. Rev. B* **96**, 115124 (2017).
- [27] E. Ilievski and J. De Nardis, Ballistic transport in the one-dimensional Hubbard model: The hydrodynamic approach, *Phys. Rev. B* **96**, 081118 (2017).
- [28] M. Fagotti, Higher-order generalized hydrodynamics in one dimension: The noninteracting test, *Phys. Rev. B* **96**, 220302 (2017).
- [29] V.B. Bulchandani, On classical integrability of the hydrodynamics of quantum integrable systems, *J. Phys. A* **50**, 435203 (2017).
- [30] B. Doyon, H. Spohn, and T. Yoshimura, A geometric viewpoint on generalized hydrodynamics, *Nucl. Phys. B* **926**, 570 (2018).
- [31] M. Collura, A. De Luca, and J. Viti, Analytic solution of the domain wall non-equilibrium stationary state, *Phys. Rev. B* **97**, 081111 (2018).
- [32] A. Bastianello, B. Doyon, G. Watts, and T. Yoshimura, Generalized hydrodynamics of classical integrable field theory: The sinh-Gordon model, *SciPost Phys.* **4**, 045 (2018).
- [33] By thermal equilibrium we mean a state represented by the Gibbs ensemble at a given temperature and chemical potential.
- [34] S. Stringari, Dynamics of Bose-Einstein condensed gases in highly deformed traps, *Phys. Rev. A* **58**, 2385 (1998).
- [35] C. Menotti and S. Stringari, Collective oscillations of one-dimensional Bose-Einstein gas in a time-varying trap potential and atomic scattering length, *Phys. Rev. A* **66**, 043610 (2002).
- [36] S. Peotta and M. Di Ventra, Quantum shock waves and population inversion in collisions of ultracold atomic clouds, *Phys. Rev. A* **89**, 013621 (2014).
- [37] I. Bouchoule, S.S. Szigeti, M.J. Davis, and K.V. Kheruntsyan, Finite-temperature hydrodynamics for one-dimensional Bose gases: Breathing-mode oscillations as a case study, *Phys. Rev. A* **94**, 051602(R) (2016).
- [38] G. De Rosi and S. Stringari, Hydrodynamic versus collisionless dynamics of a one-dimensional harmonically trapped Bose gas, *Phys. Rev. A* **94**, 063605 (2016).
- [39] Y.Y. Atas, D.M. Gangardt, I. Bouchoule, and K.V. Kheruntsyan, Exact nonequilibrium dynamics of finite-temperature Tonks-Girardeau gases, *Phys. Rev. A* **95**, 043622 (2017).
- [40] See Supplemental Material at <http://link.aps.org/supplemental/10.1103/PhysRevLett.122.090601> for a brief introduction of the Gross-Pitaevskii and the classical field models, which includes Refs. [41–45].
- [41] Y. Castin, R. Dum, E. Mandonnet, A. Minguzzi, and I. Carusotto, Coherence properties of a continuous atom laser, *J. Mod. Opt.* **47**, 2671 (2000).
- [42] I. Bouchoule, M. Arzamasovs, K.V. Kheruntsyan, and D.M. Gangardt, Two-body momentum correlations in a weakly interacting one-dimensional Bose gas, *Phys. Rev. A* **86**, 033626 (2012).
- [43] T. Jacqmin, B. Fang, T. Berrada, T. Roscilde, and I. Bouchoule, Momentum distribution of one-dimensional Bose gases at the quasicondensation crossover: Theoretical and experimental investigation, *Phys. Rev. A* **86**, 043626 (2012).
- [44] P.B. Blakie, A.S. Bradley, M.J. Davis, R.J. Ballagh, and C.W. Gardiner, Dynamics and statistical mechanics of ultracold Bose gases using c-field techniques, *Adv. Phys.* **57**, 363 (2008).
- [45] S.P. Cockburn, A. Negretti, N.P. Proukakis, and C. Henkel, A comparison between microscopic methods for finite temperature Bose gases, *Phys. Rev. A* **83**, 043619 (2011).
- [46] C.N. Yang and C.P. Yang, Thermodynamics of a one-dimensional system of bosons with repulsive delta-function interaction, *J. Math. Phys.* **10**, 1115 (1969).
- [47] A. Zamolodchikov, Thermodynamic Bethe ansatz in relativistic models. Scaling three state Potts and Lee-Yang models, *Nucl. Phys. B* **342**, 695 (1990).
- [48] J. Mossel and J.-S. Caux, Generalized TBA and generalized Gibbs, *J. Phys. A* **45**, 255001 (2012).
- [49] E. Ilievski, M. Medenjak, T. Prosen, and L. Zadnik, Quasilocal charges in integrable lattice systems, *J. Stat. Mech.* (2016) 064008.
- [50] A. Johnson, Ph.D. thesis, 2016, <https://tel.archives-ouvertes.fr/tel-01432392v1>.
- [51] K.V. Kheruntsyan, D.M. Gangardt, P.D. Drummond, and G.V. Shlyapnikov, Pair Correlations in a Finite-Temperature 1D Bose Gas, *Phys. Rev. Lett.* **91**, 040403 (2003).
- [52] M. Olshanii, Atomic Scattering in the Presence of an External Confinement and a Gas of Impenetrable Bosons, *Phys. Rev. Lett.* **81**, 938 (1998).
- [53] C. Mora and Y. Castin, Extension of Bogoliubov theory to quasicondensates, *Phys. Rev. A* **67**, 053615 (2003).

- [54] M. Cazalilla, Bosonizing one-dimensional cold atomic gases, *J. Phys. B* **37**, S1 (2004).
- [55] For each x , the initial distribution $\rho(x, v)$ is given by the thermodynamic Bethe ansatz [46].
- [56] See Supplemental Material at <http://link.aps.org/supplemental/10.1103/PhysRevLett.122.090601> for a detailed discussion of why the GHD prediction is close to the CHD one for the release from a harmonic trap.
- [57] See Supplemental Material at <http://link.aps.org/supplemental/10.1103/PhysRevLett.122.090601> for plots of the distribution of quasiparticles in phase space and more details on why the double-well potential allows to discriminate between GHD and CHD.
- [58] See Supplemental Material at <http://link.aps.org/supplemental/10.1103/PhysRevLett.122.090601> for full details on our selection procedure for the GHD profiles in the case where we do not have good knowledge of the initial potential.
- [59] T. Kinoshita, T. Wenger, and D. S. Weiss, A Quantum Newton's Cradle, *Nature (London)* **440**, 900 (2006).
- [60] Y. Tang, W. Kao, K.-Y. Li, S. Seo, K. Mallayya, M. Rigol, S. Gopalakrishnan, and B. L. Lev, Thermalization near Integrability in a Dipolar Quantum Newton's Cradle, *Phys. Rev. X* **8**, 021030 (2018).
- [61] C. Li, T. Zhou, I. Mazets, H.-P. Stimming, Z. Zhu, Y. Zhai, W. Xiong, X. Zhou, X. Chen, and J. Schmiedmayer, Dephasing and relaxation of bosons in 1D: Newton's cradle revisited, [arXiv:1804.01969](https://arxiv.org/abs/1804.01969).
- [62] See Supplemental Material at <http://link.aps.org/supplemental/10.1103/PhysRevLett.122.090601> for plots of the distribution of quasiparticles in phase space that show that the behavior predicted by GHD is only approximately periodic.
- [63] To go beyond the shock time, one would need to properly regularize the solution, for instance, by considering entropy-producing diffusive terms.
- [64] C. N. Yang, Some Exact Results for the Many-Body Problem in one Dimension with Repulsive Delta-Function Interaction, *Phys. Rev. Lett.* **19**, 1312 (1967).
- [65] B. Sutherland, Further Results for the Many-Body Problem in One Dimension, *Phys. Rev. Lett.* **20**, 98 (1968).
- [66] M. Gaudin, Un système a une dimension de fermions en interaction, *Phys. Lett.* **24A**, 55 (1967).
- [67] X.-W. Guan, M. Batchelor, and C. Lee, Fermi gases in one dimension: From Bethe ansatz to experiments, *Rev. Mod. Phys.* **85**, 1633 (2013).
- [68] P. Wicke, S. Whitlock, and N. van Druten, Controlling spin motion and interactions in a one-dimensional Bose gas, [arXiv:1010.4545](https://arxiv.org/abs/1010.4545).
- [69] G. Papagano *et al.*, A one-dimensional liquid of fermions with tunable spin, *Nat. Phys.* **10**, 198 (2014).